

University of Massachusetts Medical School

eScholarship@UMMS

---

UMass Metabolic Network Publications

UMass Metabolic Network

---

2017-11-01

## Association of Multiorgan Computed Tomographic Phenomap With Adverse Cardiovascular Health Outcomes: The Framingham Heart Study


Ravi V. Shah

*Massachusetts General Hospital*

*Et al.*

Let us know how access to this document benefits you.

Follow this and additional works at: [https://escholarship.umassmed.edu/metnet\\_pubs](https://escholarship.umassmed.edu/metnet_pubs)

 Part of the [Biochemistry Commons](#), [Cardiology Commons](#), [Cardiovascular Diseases Commons](#), [Cell Biology Commons](#), [Cellular and Molecular Physiology Commons](#), and the [Molecular Biology Commons](#)

---

### Repository Citation

Shah RV, Yeri AS, Murthy VL, Massaro JM, D'Agostino RS, Freedman JE, Long MT, Fox CS, Das S, Benjamin EJ, Vasan RS, O'Donnell CJ, Hoffmann U. (2017). Association of Multiorgan Computed Tomographic Phenomap With Adverse Cardiovascular Health Outcomes: The Framingham Heart Study. UMass Metabolic Network Publications. <https://doi.org/10.1001/jamacardio.2017.3145>. Retrieved from [https://escholarship.umassmed.edu/metnet\\_pubs/151](https://escholarship.umassmed.edu/metnet_pubs/151)

This material is brought to you by eScholarship@UMMS. It has been accepted for inclusion in UMass Metabolic Network Publications by an authorized administrator of eScholarship@UMMS. For more information, please contact [Lisa.Palmer@umassmed.edu](mailto:Lisa.Palmer@umassmed.edu).

# Association of Multiorgan Computed Tomographic Phenomap With Adverse Cardiovascular Health Outcomes

## The Framingham Heart Study

Ravi V. Shah, MD; Ashish S. Yeri, PhD; Venkatesh L. Murthy, MD, PhD; Joe M. Massaro, PhD; Ralph D'Agostino Sr, PhD; Jane E. Freedman, MD; Michelle T. Long, MD; Caroline S. Fox, MD, MHS; Saumya Das, MD, PhD; Emelia J. Benjamin, MD, ScM; Ramachandran S. Vasan, MD; Christopher J. O'Donnell, MD, MPH; Udo Hoffmann, MD, MPH

 Supplemental content

**IMPORTANCE** Increased ability to quantify anatomical phenotypes across multiple organs provides the opportunity to assess their cumulative ability to identify individuals at greatest susceptibility for adverse outcomes.

**OBJECTIVE** To apply unsupervised machine learning to define the distribution and prognostic importance of computed tomography–based multiorgan phenotypes associated with adverse health outcomes.

**DESIGN, SETTING, AND PARTICIPANTS** This asymptomatic community-based cohort study included 2924 Framingham Heart Study participants between July 2002 and April 2005 undergoing computed tomographic imaging of the chest and abdomen. Participants are from the offspring and third-generation cohorts.

**EXPOSURES** Eleven computed tomography–based measures of valvular/vascular calcification, adiposity, and muscle attenuation.

**MAIN OUTCOMES AND MEASURES** All-cause mortality and cardiovascular disease (myocardial infarction, stroke, or cardiovascular death).

**RESULTS** The median age of the participants was 50 years (interquartile range, 43-60 years), and 1422 (48.6%) were men. Principal component analysis identified 3 major anatomic axes: (1) global calcification (defined by aortic, thoracic, coronary, and valvular calcification); (2) adiposity (defined by pericardial, visceral, hepatic, and intrathoracic fat); and (3) muscle attenuation that explained 65.7% of the population variation. Principal components showed different evolution with age (continuous increase in global calcification, decrease in muscle attenuation, and U-shaped association with adiposity) but similar patterns in men and women. Using unsupervised clustering approaches in the offspring cohort (n = 1150), we identified a cohort (n = 232; 20.2%) with an unfavorable multiorgan phenotype across all 3 anatomic axes as compared with a favorable multiorgan phenotype. Membership in the unfavorable phenotypic cluster was associated with a greater prevalence of cardiovascular disease risk factors and with increased all-cause mortality (hazard ratio, 2.61; 95% CI, 1.74-3.92;  $P < .001$ ), independent of coronary artery calcium score, visceral adipose tissue, and 10-year global cardiovascular disease Framingham risk, and it provided improvement in metrics of discrimination and reclassification.

**CONCLUSIONS AND RELEVANCE** This proof-of-concept analysis demonstrates that unsupervised machine learning, in an asymptomatic community cohort, identifies an unfavorable multiorgan phenotype associated with adverse health outcomes, especially in elderly American adults. Future investigations in larger populations are required not only to validate the present results, but also to harness clinical, biochemical, imaging, and genetic markers to increase our understanding of healthy cardiovascular aging.

JAMA Cardiol. 2017;2(11):1236-1246. doi:10.1001/jamacardio.2017.3145  
Published online September 20, 2017.

**Author Affiliations:** Author affiliations are listed at the end of this article.

**Corresponding Author:** Udo Hoffmann, MD, MPH, Cardiac MR PET CT Program, Massachusetts General Hospital, 165 Cambridge St, Boston, MA 02114 (uhoffmann@mgh.harvard.edu).

Cardiovascular disease (CVD) is the result of unfavorable changes in structure and function across multiple organ systems.<sup>1-3</sup> Seminal investigations have detailed the importance of many individual phenotypes physiologically central to CVD, including coronary<sup>4-7</sup> and valvular<sup>8</sup> calcification, adiposity (eg, abdominal visceral and pericardial fat depots),<sup>9-14</sup> muscle fat content, and sarcopenia.<sup>15-17</sup> Although these individual CVD-related phenotypes may be associated with each other, their presence and extent vary substantially between individuals: individuals with coronary vascular calcification may not have valvular or abdominal aortic calcification (and vice versa), likely owing to distinct genetic/epigenetic determinants.<sup>18</sup> Thus, while coronary calcification is a strong marker of CVD risk, a phenotype spanning multiple organs (similar to multimarker blood biomarker approaches<sup>19</sup>) may be important to understand which individuals are at greatest susceptibility for adverse CVD-related prognosis.

Recently, machine learning techniques have been used to summarize and classify multiple phenotypes and outcomes in CVD (phenomapping),<sup>20</sup> although the clinical or physiologic value of such approaches in CVD remains unclear.<sup>21</sup> In this study, we examined 2924 participants of the Framingham Heart Study (FHS) offspring and third-generation cohorts with computed tomographic (CT) measurements of 11 different organ phenotypes across the chest and abdomen, including vascular and cardiac calcification and adipose and muscle tissue characteristics. Using a machine learning approach, we sought to describe patterns of variation of presence and extent of individual phenotypes across vascular and valvular calcification; abdominal, intrathoracic, and pericardial adiposity; and liver and muscle fat content. Furthermore, we wanted to understand whether combining information from these phenotypes would identify prognostically and phenotypically distinct subgroups within a heterogeneous population.

## Methods

### Study Cohort and Imaging Exposures

The analytic cohort comprised participants in the FHS offspring cohort (n = 1150; median age, 63 years; interquartile range [IQR], 57-70 years; age range, 40-87 years; 57% female) or the third-generation cohort (n = 1774; median age, 45 years; IQR, 40-49 years; age range, 32-72 years; 48% female) who underwent chest and abdominal CT imaging between 2002 and 2005. We included 2924 individuals with available measures for all imaging domains assayed (calcification, adiposity, and liver and muscle attenuation; eFigure 1 in the [Supplement](#)). Techniques for quantification of the various calcification<sup>8</sup> and fat<sup>10,22</sup> phenotypes have been previously described and are detailed in eTable 1 in the [Supplement](#). The study design and methods for data collection have been published elsewhere.<sup>23</sup> The institutional review boards of Boston University Medical Center and Massachusetts General Hospital approved the study. All participants provided written informed consent.

## Key Points

**Question** Can an unbiased evaluation of multiorgan phenotypes identify favorable and unfavorable clusters within a community-based cohort, especially among elderly American adults?

**Findings** Using 11 quantitative computed tomography-based phenotypes, this cohort study found that unsupervised machine learning identified a favorable multiorgan phenotype characterized by increased calcification, adiposity, and muscle fat, which was associated with a 2-fold increased hazard of death at 10 years, robust to adjustment for age, sex, risk factors, and individual phenotypes.

**Meaning** This proof-of-concept analysis demonstrates that unsupervised machine learning identifies an unfavorable multiorgan phenotype associated with adverse health outcomes, especially in elderly American adults.

### Cardiovascular and Noncardiovascular Mortality

All-cause mortality was our primary outcome. We included hard CVD events as a secondary outcome, defined as a composite of death due to coronary heart disease or stroke, nonfatal myocardial infarction, or nonfatal ischemic stroke. Methods for adjudication of these events have been previously reported.<sup>10</sup>

### Statistical Analysis

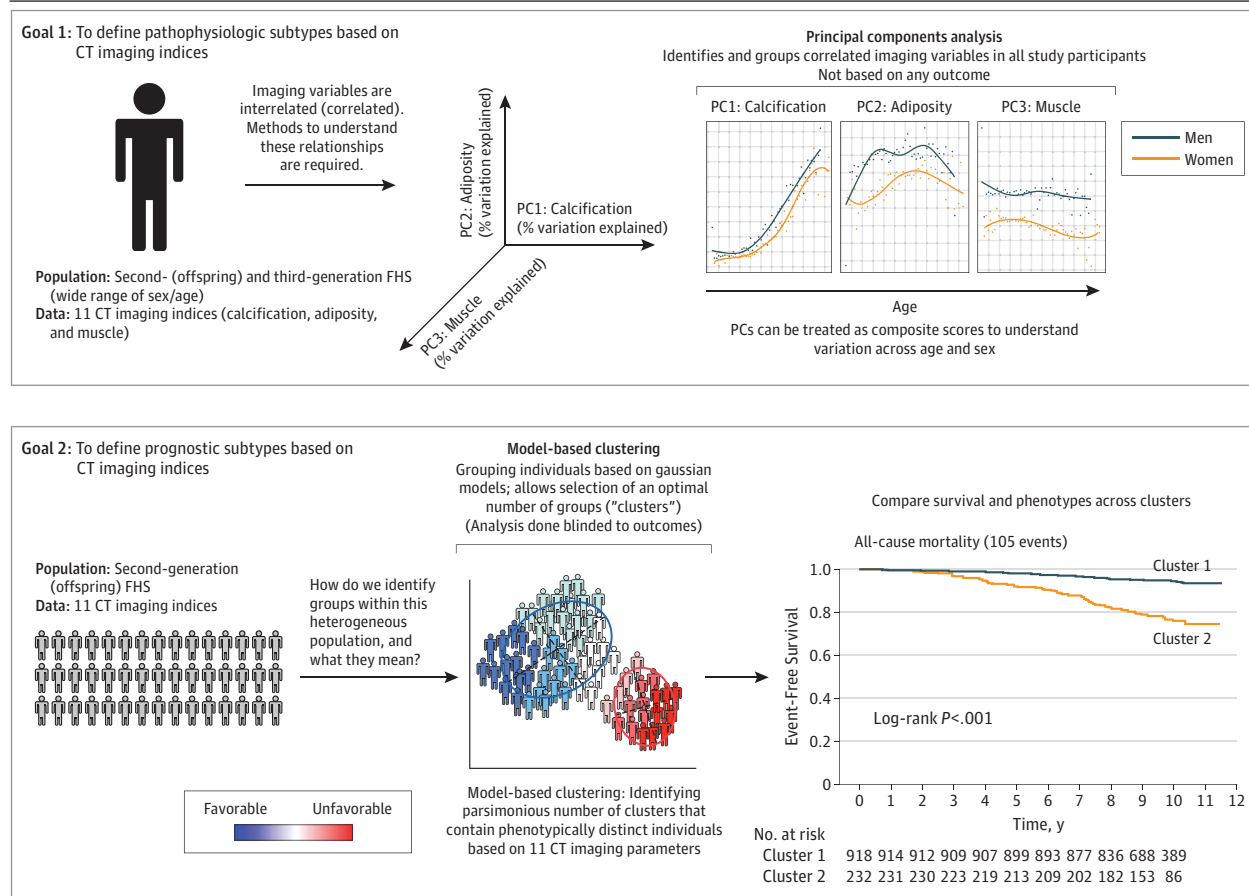
#### General Descriptive Statistics

Descriptive data were expressed as percentage (for categorical variables) or median and IQR (for continuous variables). Correlations between imaging indices were estimated using Spearman coefficients. Comparison of covariates among quartiles of age was performed via standard methods (nonparametric Wilcoxon or Kruskal-Wallis tests for continuous and  $\chi^2$  test for categorical variables).

#### General Approach

The overall goal of our study was in 2 phases ([Figure 1](#)). First, we sought to describe patterns of variation in 11 CT phenotypes across vascular and valvular calcification; abdominal, intrathoracic, and pericardial adiposity; and liver and muscle fat content. For this first step, we used a principal components analysis (PCA), an unsupervised learning technique that statistically groups correlated phenotypes together into components; each of these components accounts for some proportion of variation in overall data. These components can then be used to understand interrelationships among imaging variables and their variability across age and sex in the FHS. Second, we wanted to understand whether CT phenotypes would be able to classify participants in the FHS offspring cohort into prognostically and phenotypically distinct subgroups. For this second step, we used a clustering technique that identified clusters of participants based on all 11 CT phenotypes. The 2 approaches (PCA and clustering) were chosen to address specific hypotheses in our study and are not related. We have specified the details of each method in this section.

Figure 1. Unsupervised Machine Learning to Define Unique Phenotypic Subtypes



Schematic of study design. Unsupervised machine learning refers to methods that define associations without relying on a predetermined outcome (eg, death and cardiovascular disease events). CT indicates computed tomography; FHS, Framingham Heart Study; and PC, principal component.

**Principal Components Analysis**

To cover the broadest range of age in FHS, we used all 2924 participants (offspring and third-generation cohorts) in our descriptive analysis by PCA. Before entry into PCA, all imaging variables were natural log-transformed to reduce variance, followed by mean centering and standardization (mean, 0; variance, 1). A value of 1 was added to each calcification variable (coronary, aortic, thoracic, and valvular) before log-transformation to allow estimation of the logarithm for zero calcification values. The adiposity and liver and muscle fat variables were log-transformed. The total number of principal components (PCs) to include in our analysis was determined by scree plot and inclusion of PCs up to 60% of the overall variance. Varimax rotation was used to determine final PC loadings. We examined the distribution of PC-based scores using a box plot for each decade of age for men and women separately. We measured the association of age and sex with PC scores using a linear model with inclusion of a quadratic term for age (to model nonlinearity). Effect modification by sex was assessed using a multiplicative interaction term between age and sex in each model.

**Clustering**

We chose to focus on the offspring cohort for the clustering analysis for several reasons. First, our primary research interest was to investigate an older, at-risk population with a greater prevalence (and incidence) of disease, in which imaging indices may have a greater impact on differentiating disease subsets. Second, the 2 cohorts (the second generation or offspring cohort vs third generation) aged in different eras of medical care, leading to potential unmeasured differences in prevention and surveillance. To visualize the data, we first performed unsupervised agglomerative hierarchical clustering, with the Manhattan distance measure more robust in terms of assigning cluster and the Ward method of clustering using all 11 imaging indices (log-transformed, mean centered, and standardized, as with PCA), in 1150 offspring cohort participants. Clusters were plotted as a heatmap using a modified version of *heatmap.2* (package *hclust* in R) to include bars for all-cause mortality and incident CVD. While hierarchical clustering is sufficient for the purposes of visualization, it is difficult to accurately classify the participants into different clusters. Model-based clustering is more robust in terms of assigning clusters to data that are

either overlapping or have varying sizes or shapes. To accurately classify the 1150 participants into clusters, we used a gaussian model-based clustering to identify the optimal number of clusters within our data. In this approach, each cluster is modeled as a gaussian multivariate mixture model with a mean and covariance that describes its shape. The *mclust* package in R<sup>24</sup> fits a variety of gaussian mixture models to the observed data, followed by identification of the optimal number of clusters using an information criterion (eg, Bayesian information criterion) that penalizes model complexity based on the number of clusters. For a full list of models investigated, refer to eFigure 2 in the [Supplement](#).

#### Cluster Validation

We performed internal validation within the offspring cohort to evaluate fitting of the model-based clustering. As previously noted, model-based clustering allocated FHS participants in 1 of 2 groups: a favorable cluster (cluster 1) and an unfavorable cluster (cluster 2). To determine the robustness of the cluster membership, we performed logistic regression with 100 naive bootstraps. Here, the dependent (predictor) variable is cluster membership (cluster 1 or cluster 2). The independent variables are the 11 imaging indices. Briefly, approximately 62% of the individuals in the overall cohort of 1150 were randomly selected, with replacement in each bootstrap, and a logistic regression model is built using the *glm* and *caret* package in R. The remaining approximate 38% of the samples are introduced into this model and the performance metrics (accuracy, sensitivity, and specificity) of the logistic regression model are evaluated. This process is repeated for 100 random splits of the population. The model prediction from the logistic regressions in 100 bootstraps is subsequently used to compute the area under the receiver operating characteristic curve (C-statistic) with 95% CIs using the *pROC* package in R.

To identify clinical determinants of cluster membership, we compared clinical and demographic characteristics between the 2 identified clusters using Wilcoxon (continuous) and  $\chi^2$  (categorical) statistics. The cluster optimization approach used here has been widely used in machine learning applied to genomics and has been used in deep clinical phenotyping.<sup>20</sup>

#### Event Analysis

After generating clusters of phenotypically distinct participants in the offspring cohort, we determined the association of membership in a given cluster with outcomes. We estimated Cox regression models for each specified outcome (primary: all-cause mortality; secondary: hard CVD) as a function of cluster membership, adjusted for 10-year global Framingham CVD risk as an age- and sex-specific marker of cardiovascular risk. We additionally adjusted for coronary artery calcium score (modeled at  $\log[\text{CAC}+1]$ ) and visceral adipose tissue (log-transformed) in multivariable models to assess whether composite imaging phenotypes (as identified in cluster membership) would be associated with outcome independently of single prognostic measures of calcification and fat, respectively. Proportional hazards were confirmed for each model using the supremum test. Finally, to assess incremen-

tal prognostic value of cluster membership over clinical risk (by 10-year Framingham risk) and imaging-based risk (by coronary calcium and visceral adiposity), we calculated a C-index for each model (comparing C-indices by established methods<sup>25</sup>) and a continuous net reclassification index (NRI) and relative integrated discrimination improvement (IDI).<sup>26</sup> Confidence intervals for NRI and IDI were computed by bootstrapping with 999 resamples. The NRI and C-index were computed at a point selected between the median and 75th percentile of follow-up duration to optimize balance between power and bias (at 10.0 years for all-cause mortality and 9.5 years for CVD).

All statistics were performed in SAS version 9.3 (SAS Institute) or R version 3.3.1 (R Foundation). A 2-tailed  $P < .05$  was used as a criteria for significance.

## Results

### Study Population

An overview of the cohort is shown in eFigure 1 in the [Supplement](#). The characteristics of the study population (by quartiles) are shown in [Table 1](#). Of the 2924 FHS participants, 1150 were members of the offspring cohort and 1774 members of the third-generation cohort. The median age of the overall cohort was 50 years (IQR, 43-60 years), 48.6% were men, and the mean 10-year CVD risk (by the 10-year Global CVD Framingham risk as described<sup>27</sup>) was 4.9%. Of note, the 558 participants who were excluded from the study had a generally higher cardiometabolic risk (eTable 2 in the [Supplement](#)).

### Distinct Components of Variability in Multiorgan CT Phenotypes

We observed statistically significant but modest correlations among calcification parameters (eg, for coronary calcification; Spearman  $\rho$  range, 0.07-0.62; eFigure 3 in the [Supplement](#)). On the other hand, we observed highest correlation between regional fat measures (eg, visceral vs intrathoracic fat, Spearman  $\rho = 0.86$ ). Given the significant differences in interrelationships across imaging parameters, we used PCA to visualize how each individual imaging phenotype naturally grouped together.<sup>28</sup> Three PCs described 65.7% of the overall variation in imaging measures ([Figure 2A](#); scree plot in eFigure 4 in the [Supplement](#)). Principal component 1 was highly associated with coronary, valvular, and noncoronary vascular calcification indices; therefore, we termed PC1 a global (valvular/vascular) calcification PC. Principal component 2 identified adiposity component, with positive association with visceral, pericardial, subcutaneous, hepatic, and intrathoracic fat. Finally, we labeled PC3 as a muscle quality component, given that we observed the highest loading on muscle attenuation in this PC (with greater values of attenuation corresponding to decreased intramuscular fat). The dependence of each PC score on age and sex is depicted in [Figure 2B](#). We found significant nonlinearity in PC scores by age for all PCs ( $\text{age}^2$ :  $P < .05$  for all PCs). In general, we observed an increase in valvular/vascular calcification with age ( $\text{PC1-age} + \text{age}^2 + \text{sex}$ ,  $\beta_{\text{age}} = -1.05, P < .05$ , and  $\beta_{\text{age}^2} = -1.5 \times 10^{-3}, P < .05$ ), a more complex (U-shaped) association with adiposity with age ( $\text{PC2-age} + \text{age}^2 + \text{sex}$ ,  $\beta_{\text{age}} = 0.14, P < .05$ , and  $\beta_{\text{age}^2} = -1.1 \times 10^{-3}, P < .05$ ),



Table 1. Characteristics of 2924 Framingham Heart Study Participants, Stratified by Quartile of Age

Characteristic	Study Cohort (N = 2924)	Quartile 1 (Age 32-43 y) <sup>a</sup> (n = 757)	Quartile 2 (Age 44-49 y) <sup>a</sup> (n = 655)	Quartile 3 (Age 50-60 y) <sup>a</sup> (n = 785)	Quartile 4 (Age 61-87 y) <sup>a</sup> (n = 727)
<b>Baseline Demographics</b>					
Age at CT examination, median (IQR), y	50.0 (43.0-60.0)	40.0 (38.0-42.0)	46.0 (45.0-48.0)	54.0 (51.0-57.0)	68.0 (64.0-74.0)
Male, No. (%)	1422 (48.6)	462 (61.0)	303 (46.3)	352 (44.8)	305 (42.0)
Current smoker, No. (%)	382 (13.1)	124 (16.4)	98 (15.0)	118 (15.0)	42 (5.8)
Antihypertensive therapy use, No. (%)	518 (17.7)	40 (5.3)	63 (9.6)	148 (18.9)	267 (36.7)
Lipid-lowering therapy use, No. (%)	364 (12.5)	50 (6.6)	57 (8.7)	96 (12.2)	161 (22.2)
Offspring cohort	1150 (39.3)	10 (1.3)	52 (7.9)	387 (49.3)	701 (96.4)
Third-generation cohort	1774 (60.7)	747 (98.7)	603 (92.1)	398 (50.7)	26 (3.6)
History of CVD, No. (%)	52 (1.8)	0 (0)	2 (0.3)	13 (1.7)	37 (5.1)
<b>Cardiometabolic Risk Factors</b>					
BMI, median (IQR) (n = 2923)	26.7 (23.8-30.1)	25.9 (23.0-29.2)	26.4 (23.3-29.9)	27.0 (24.2-30.1)	27.5 (24.8-31.2)
Waist circumference, median (IQR), cm (n = 2921)	95.3 (86.4-104.14)	91.4 (58.4-100.3)	94.0 (85.1-104.1)	96.5 (87.6-105.4)	99.1 (91.4-108.7)
Framingham risk score, median (IQR), % (n = 2923)	4.9 (2.7-8.6)	2.8 (1.4-4.7)	3.8 (2.1-6.0)	5.8 (3.5-9.0)	9.3 (5.8-15.4)
Diabetes, No. (%)	166 (5.7)	17 (2.3)	17 (2.6)	46 (5.9)	86 (11.8)
Hypertension, No. (%)	811 (27.7)	102 (13.5)	115 (17.6)	230 (29.3)	364 (50.1)
Blood pressure, median (IQR), mm Hg					
Systolic (n = 2923)	120.0 (110.0-130.0)	115.0 (107.0-123.0)	118.0 (109.0-126.0)	121.0 (111.0-130.0)	127.0 (117.0-141.0)
Diastolic (n = 2920)	76.0 (69.0-82.0)	76.0 (69.0-82.0)	76.0 (71.0-82.0)	77.0 (70.0-83.0)	73.0 (67.0-80.0)
Cholesterol level, median (IQR), mg/dL					
Total	194.0 (173.0-218.0)	187.0 (167.0-210.0)	190.0 (170.0-214.0)	200.0 (176.0-223.0)	198.0 (177.0-224.0)
HDL	52.0 (42.0-64.0)	50.0 (41.0-60.0)	53.0 (42.0-65.0)	54.0 (43.0-67.0)	52.0 (42.0-63.0)
Triglyceride level, median (IQR), mg/dL	101.0 (71.0-153.0)	90.0 (65.0-137.0)	94.0 (67.0-145.0)	101.0 (73.0-150.0)	120.0 (81.0-175.0)
<b>Imaging Parameters</b>					
Calcification, median (IQR) <sup>b</sup>					
Thoracic aortic	0 (0-0)	0 (0-0)	0 (0-0)	0 (0-0)	53.9 (0-397.8)
Coronary artery	0 (0-44.1)	0 (0-0)	0 (0-1.0)	0 (0-43.4)	82.0 (3.9-409.5)
Abdominal aortic	3.9 (0-513.1)	0 (0-0)	0 (0-30.0)	30.4 (0-444.3)	1304.2 (255.1-3389.1)
Aortic valve	0 (0-0)	0 (0-0)	0 (0-0)	0 (0-0)	0 (0-50.9)
Mitral valve	0 (0-0)	0 (0-0)	0 (0-0)	0 (0-0)	0 (0-3.8)
Intrathoracic fat, median (IQR), mL	80.5 (49.2-124.1)	63.9 (37.8-101.2)	68.9 (39.2-114.5)	83.6 (54.3-126.5)	105.3 (71.6-150.8)
Pericardial fat, median (IQR), mL	102.9 (80.0-132.8)	90.6 (71.5-116.9)	98.2 (76.7-124.9)	106.1 (83.2-134.9)	120.1 (93.4-152.9)
VAT, median (IQR), mL	1594.1 (925.6-2330.8)	1305.3 (727.4-1874.2)	1418.0 (803.9-2213.4)	1656.0 (992.1-2378.1)	1975.0 (1353.3-2788.5)
Liver attenuation, median (IQR), HU	68.0 (63.3-71.3)	68.3 (64.7-71.3)	68.0 (63.3-71.3)	68.0 (62.7-71.0)	67.3 (62.0-71.0)
SAT, median (IQR), mL	2561.1 (1866.8-3525.8)	2182.2 (1619.9-3026.8)	2528.9 (1780.6-3538.5)	2725.8 (1988.9-3766.7)	2771.3 (2113.7-3677.2)
Muscle attenuation, median (IQR), HU	57.5 (53.5-60.5)	60.5 (58.0-62.5)	58.5 (56.0-60.5)	57.0 (53.5-59.5)	52.0 (47.5-55.5)

Abbreviations: BMI, body mass index (calculated as weight in kilograms divided by height in meters squared); CT, computed tomography; CVD, cardiovascular disease; HDL, high-density lipoprotein; HU, Hounsfield units; IQR, interquartile range; SAT, subcutaneous adipose tissue; VAT, visceral adipose tissue.

levels to millimoles per liter, multiply by 0.0259.

<sup>a</sup> Age ranges signify the minimum and maximum age at CT scan in each quartile of age.

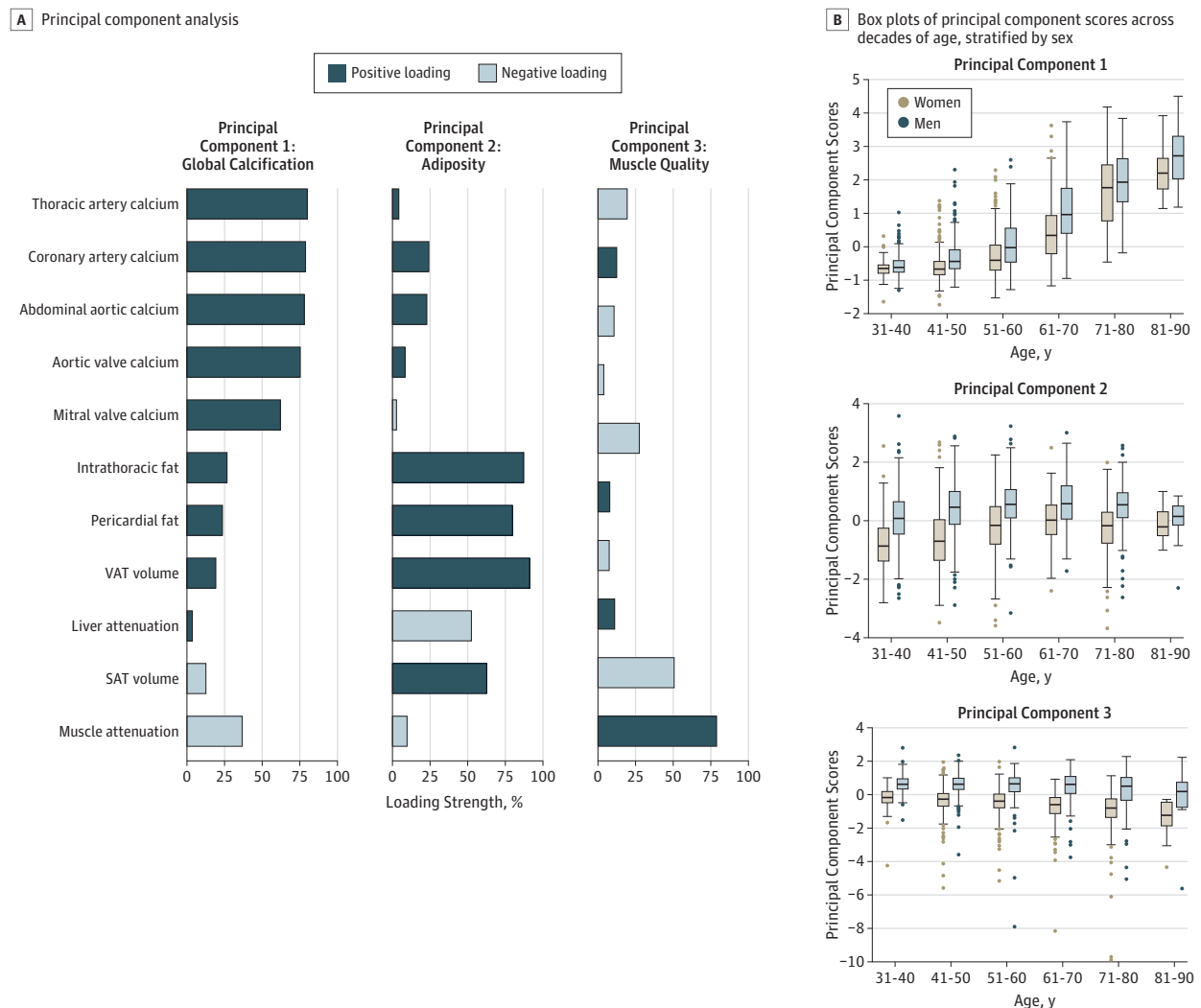
<sup>b</sup> Units for calcification measures are as described in eTable 1 in the Supplement.

SI conversion factors: To convert HDL and total cholesterol and triglyceride

and a gradual decline in muscle quality with age (PC3-age + age<sup>2</sup> + sex,  $\beta_{age} = -0.03$ ,  $P < .05$ , and  $\beta_{age^2} = 4.5 \times 10^{-4}$ ,  $P < .05$ ). While we observed a significant association of each

PC score with sex ( $P < .05$  for all; men with higher calcification and adiposity; lower muscle fat), only the association between global calcification (PCI) and age was modified by sex

Figure 2. Principal Components Analysis



Principal components analysis of 11 parameters obtained from chest and abdominal computed tomographic imaging. A, Three principal components (representing 65.7% of the total variance in the imaging data) with loadings of each imaging parameter are presented. The dark blue hue represents imaging variables that have positive loading in a given principal component; the light blue hue represents imaging variables that have a negative loading in a given principal component. Of note, greater liver or muscle attenuation corresponds

to decreased liver or intramuscular fat, respectively; therefore, a positive loading for muscle in principal component 3 signifies that a higher principal component 3 score is associated with greater muscle attenuation (lower intramuscular fat content). B, Box plots of principal component scores across decades of age. Details of statistical testing are specified in the text. SAT indicates subcutaneous adipose tissue; VAT, visceral adipose tissue.

(PC1-age + age<sup>2</sup> + sex + age × sex + age<sup>2</sup> × sex,  $\beta_{\text{age} \times \text{sex}} = 0.06$ ,  $P < .05$ , and  $\beta_{\text{age}^2 \times \text{sex}} = -4.7 \times 10^{-4}$ ,  $P < .05$ ).

### Phenotypically Distinct Groups of Older American Adults

Our next step was to use the 11 different imaging phenotypes to understand underlying groups within the offspring cohort with different physiology and prognosis. Based on the hierarchical clustering of the 11 imaging variables, we observed 2 main clusters, with concordance between high calcification and adiposity parameters in individuals at highest risk of death or CVD of individuals with high calcification and fat (eFigure 5 in the Supplement). To accurately classify indi-

viduals into the highest-risk group, we used a model-based clustering to get 2 phenotypically distinct clusters. Gaussian model-based clustering revealed 2 distinct clusters of participants in the offspring cohort. The model selected by the package *mclust* was an ellipsoidal, equal volume and orientation with 2 components or clusters (eFigure 2 in the Supplement).

To determine whether the model-based clustering was overfit, we performed internal validation using logistic regression (described in Cluster Validation in the Methods section). A logistic regression model (dependent variable: cluster membership; independent variables: 11 imaging indices) with 100 naive bootstraps yielded a C-statistic of 0.995 (95% CI, 0.994-

**Table 2. Demographics and CVD Risk Factor, Individual Phenotypes, and Adverse Events by Cluster Designation**

Variable	No. (%)		P Value
	Cluster 1: Favorable Cluster (n = 918)	Cluster 2: Unfavorable Cluster (n = 232)	
<b>Demographics and CVD Risk Factors</b>			
Age, median (IQR), y	61 (56-68)	72 (66-77)	<.001
Age > 70 y	180 (20)	144 (62)	<.001
Male	393 (43)	100 (43)	.94
10-y Framingham risk score	6.8 (4.0-11.6)	9.9 (6.2-15.9)	<.001
Smoking	100 (11)	16 (7)	.07
History of CVD <sup>a</sup>	26 (3)	19 (8)	<.001
Use of antihypertensive medication	223 (24)	105 (45)	<.001
Use of lipid-lowering therapy	132 (14)	61 (26)	<.001
Diabetes	66 (7)	35 (15)	<.001
Blood pressure, mm Hg			
Systolic	122 (111-134)	130 (119-143)	<.001
Diastolic	75 (69-81)	73 (66-80)	.04
BMI	27.2 (24.5-30.1)	28.3 (25.1-31.9)	.001
Waist circumference, cm <sup>b</sup>	97.3 (88.9-106.2)	101.6 (92.7-110.7)	<.001
Cholesterol level, mg/dL			
HDL	53 (43-64)	50 (42-60)	.05
Total	198 (177-223)	201 (183-224)	.36
Triglyceride level, mg/dL	109 (76-162)	129 (89-183)	<.001
<b>Individual Phenotypes</b>			
Adipose tissue, median (IQR), mL			
Visceral	1808.5 (1174.9-2559.9)	2165.9 (1455.8-2896.6)	<.001
Subcutaneous	2723.9 (2069.3-3655.0)	2943.8 (2040.3-3791.9)	.37
Fat, median (IQR), mL			
Pericardial	108.1 (86.0-142.5)	124.2 (97.5-155.1)	<.001
Intrathoracic	93.5 (65.2-137.8)	110.5 (79.1-156.9)	<.001
Attenuation, median (IQR), HU			
Liver	68 (63-71)	67 (61-71)	.03
Muscle	54 (50-58)	51 (45-55)	<.001
Calcification, median (IQR)			
Thoracic aortic	0 (0-73)	172 (7-1296)	<.001
Aortic valve	0 (0-1.2)	33 (1-134)	<.001
Mitral valve	0 (0-0)	57 (14-297)	<.001
Coronary artery	12 (0-141)	212 (53-683)	<.001
Abdominal aortic	292 (2-1490)	2577 (671-5000)	<.001
<b>Adverse Events</b>			
CVD	36 (4)	29 (13)	<.001
Mortality	52 (6)	53 (23)	<.001

Abbreviations: BMI, body mass index (calculated as weight in kilograms divided by height in meters squared); CVD, cardiovascular disease; HDL, high-density lipoprotein; HU, Hounsfield units; IQR, interquartile range.

SI conversion factors: To convert HDL and total cholesterol and triglyceride levels to millimoles per liter, multiply by 0.0259.

<sup>a</sup> History of CVD was defined as prior myocardial infarction or stroke.

<sup>b</sup> All measures available on all participants, except with waist circumference (n = 1 missing).

0.996) for the discrimination of cluster membership, suggesting stability of the assignment of the individuals to the 2 clusters in the offspring cohort.

The model-based clustering yielded 2 clusters within the offspring cohort: cluster 1 (a favorable phenotypic cluster) that had a more salutatory profile across all major imaging indices relative to cluster 2 (an unfavorable phenotypic cluster), including decreased visceral (but not subcutaneous) adiposity, muscle fat, and calcification (eFigure 6 in the [Supplement](#); [Table 2](#)). We found significant differences in CVD risk factors and adverse health outcomes between these clusters. Most in-

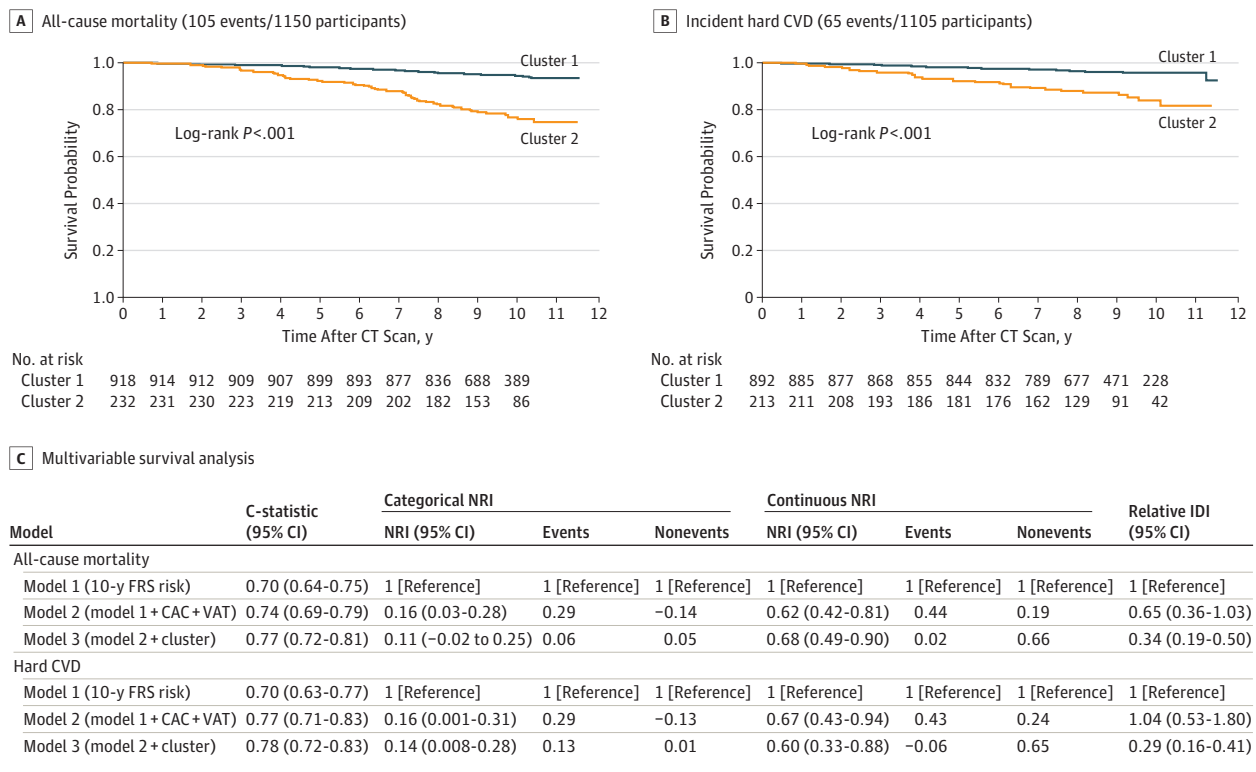
dividuals were in the favorable phenotypic cluster (cluster 1; n = 918; 79.8%). On average, members of the favorable phenotypic cluster were younger with a lower body mass index and lower prevalence of cardiovascular risk factors relative to the unfavorable cluster.

### Association of Cluster Membership With Outcome

With a median follow-up for all-cause death of 9.6 years (IQR, 8.9-10.5 years) after the CT scan, we observed 105 deaths (in 1150 individuals; 53 of 232 in the unfavorable cluster) and



Figure 3. Survival Analysis



Kaplan-Meier survival curves for all-cause mortality (A) and hard cardiovascular disease (CVD) (B) by cluster group. C, Results of multivariable survival analysis (as described in the Methods section). "Reference" indicates the referent group.

CAC indicates coronary artery calcium; CT, computed tomography; FRS, Framingham risk score; IDI, integrated discrimination improvement; NRI, net reclassification index; and VAT, visceral adipose tissue.

65 CVD events (in 1105 participants without history of CVD; 29 of 213 in the unfavorable cluster). In multivariable Cox regression adjusted for 10-year global CVD Framingham risk, membership in the unfavorable phenotypic cluster was associated with a greater than 3-fold increased hazard of all-cause mortality (hazard ratio, 3.48; 95% CI, 2.35-5.17;  $P < .001$ ), which remained significant after further adjustment for coronary artery calcium and visceral adipose tissue (hazard ratio, 2.61; 95% CI, 1.74-3.92;  $P < .001$ ). Addition of cluster membership to 10-year global CVD Framingham risk, coronary artery calcium score, and visceral adiposity was associated with a significant improvement in risk discrimination (relative IDI, 0.34; 95% CI, 0.19-0.50) and net risk reclassification (by continuous NRI; Figure 3).

For hard CVD (median follow-up, 9.0 years; IQR, 7.7-9.9 years), unfavorable cluster membership was associated with a 3-fold increased hazard (hazard ratio, 3.02; 95% CI, 1.83-4.98;  $P < .001$ ) after adjustment for 10-year Framingham risk, which attenuated but remained significant after further adjustment for coronary artery calcium score and visceral fat (hazard ratio, 2.15; 95% CI, 1.29-3.58;  $P = .003$ ). Addition of cluster membership improved discrimination (by relative IDI) and risk reclassification, driven primarily by successful reclassification of individuals without CVD events (with continuous NRI; improved specificity).

## Discussion

The primary aim of our study was to describe patterns in variability in multiorgan CT-based imaging phenotypes and whether these phenotypes could identify meaningful subgroups with different pathology and prognosis. We found modest associations between regional calcification measures and greater associations among fat measures, motivating efforts to integrate calcification and fat. Using unsupervised machine learning techniques, we uncovered 3 major anatomic components of risk—global vascular/valvular calcification, adiposity, and muscle fat content—variable by age and sex. Focusing on an older subgroup (offspring cohort), we used model-based clustering with the 11 CT imaging indices to identify 2 different clusters. Cluster membership was robust to internal cross-validation by binary logistic regression within our cohort. Each cluster had distinct clinical characteristics, with members in the more clinically adverse cluster harboring abnormalities in all domains: calcification, adiposity, and muscle fat content. After adjustment for 10-year global Framingham CVD risk, coronary artery calcium score, and visceral adiposity, cluster membership remained associated with all-cause mortality, providing significant risk discrimination and reclassification above these single measures of adiposity, calcifica-

tion, and clinical risk. Ultimately, these results suggest that joint, global alterations in multiple organ systems that directly (eg, calcification) and indirectly (eg, adiposity and muscle) impact CVD pathogenesis translates to greatest overall clinical risk.

In recognition of the biological overlap between aging, adiposity, and CVD, there is an impetus to define biomarkers that integrate these interconnected processes for risk stratification, surveillance, and targeted therapy. Individual measures have been the focus of most studies in cardiovascular prevention to date, including diastolic function,<sup>29</sup> cardiac geometry,<sup>30</sup> vascular calcification<sup>7</sup> and stiffness,<sup>31</sup> and sarcopenic obesity.<sup>11</sup> Despite their shared impact on systemic inflammation,<sup>32</sup> the mechanistic interplay between adipose, liver, and muscle tissue abnormalities with myocardial and vascular disease in humans is only recently recognized.<sup>33-36</sup> Furthermore, although calcification in different territories may “travel together,” recent results from FHS suggest that calcification in different anatomic locations may have differential impact on cardiac and all-cause mortality.<sup>8</sup> Noncoronary calcification may also have distinct genetic determinants relative to coronary calcification.<sup>18</sup> Nevertheless, studies that provide a view of individual patient-level risk as a function of integrated CVD phenotypes remain few.

In this study, we used unsupervised machine learning techniques across more than 2900 participants in a large ongoing community-based cohort study to address this limitation. By focusing on direct measures of the cardiovascular system in a heterogeneous population, we identified distinct groups of phenotypes by PCA that reflect vascular remodeling (calcification) and metabolic dysfunction (adiposity and muscle fat), and demonstrated using cluster-based techniques that these phenotypes are able to separate older individuals at high clinical risk. Importantly, while the approaches used here were “unsupervised” (not guided by operator selection or a specific outcome), they generated a clinically plausible result: a cluster of high-risk individuals in the offspring cohort marked by abnormalities across all domains of multiorgan structure by CT and reduced survival. With the increasing availability of high-dimensional data across the biochemical, clinical, genetic, and phenotypic domain,<sup>20</sup> these results provide support for unsupervised methods to identify clinically consistent, prognostic patient subgroups that integrate multiple direct (eg, calcification) and indirect (eg, adiposity) measures of CVD. Importantly, future validation in large, diverse, multiracial/ethnic aging populations is required to substantiate the findings in this study.

Defined by joint alterations in multiple imaging-based metrics of cardiometabolic health, cluster membership was associated with all-cause mortality but not hard CVD, independent of coronary artery calcium score, visceral fat, and Framingham risk, and it provided incremental risk discrimination and reclassification. While cardiac-specific events (hard CVD) are most closely linked to coronary calcification, these findings suggest that composite, global phenotypes may be important in delineating nonorgan-specific risk, specifically in older populations. Indeed, aging represents a cumulative, systemic process impacting multiple cardiovascular and metabolic systems<sup>1-3</sup> over decades (eg, calcification,<sup>4-7</sup> sarcopenia,<sup>15-17</sup> and adiposity<sup>9-14</sup>).

Efforts to integrate these phenotypes in large populations may facilitate a better understanding of rates of aging and its antecedent determinants. In addition, deeper phenotypes that more accurately capture downstream clinical risk in older populations may target discovery efforts for pathways, therapeutics, and biomarkers of healthy and unhealthy aging. In effect, the results from this study provide support for a hypothesis that maintenance of favorable adiposity, muscle, and vascular phenotypes with age is an essential component of healthy aging, and they underscore the importance of comprehensive, contemporaneous investigations of clinical, biochemical, functional, and anatomic phenotypes to better characterize what it means to age healthily.

### Strengths and Limitations

Strengths of this study include quantitative phenotypes across the chest and abdomen in a large community-based longitudinal cohort, approximately 10 years of follow-up for clinical outcomes, and the application of unsupervised methods to assess importance and linkage of individual phenotypes. In addition, the study relied on proven high-quality methods for ascertainment of cardiovascular risk factors; imaging-based measurements of calcification; muscle, liver fat, and adipose tissues; and independent adjudication of relevant clinical outcomes by established criteria.

Nevertheless, there are several limitations based in the study design. An important limitation of this work is the lack of external validation. In this regard, further investigations are needed to reproduce and externally validate the findings in this study. For example, larger populations with a greater spectrum of risk may allow for identification of a greater number of phenotypic clusters that more finely resolve prognostically, physiologically, and phenotypically distinct subgroups. In turn, these larger studies would benefit from precision molecular phenotyping (eg, metabolomewide, transcriptomewide, or proteomewide) to pinpoint mechanisms by which these structural changes interact to produce outcomes. Moreover, we did not have the opportunity to evaluate noncardiovascular elements of organ aging (eg, neurologic). Finally, the FHS cohort is of European ancestry and largely residing in Massachusetts, limiting generalizability to other races/ethnicities.

### Conclusions

Unsupervised machine learning techniques rooted in 11 quantitative, CT-based phenotypes of CVD in the chest and abdomen identified 3 important imaging-based domains (global vascular/valvular calcification, adiposity, and muscle fat). Furthermore, these 11 metrics classified offspring cohort participants into 2 phenotypically distinct clusters, with association with all-cause mortality independent of single anatomic measures of fat or coronary artery calcium score and clinical risk. Further validation of these results in larger multiracial/ethnic populations and integration with clinical, biochemical, imaging, and genetic markers are necessary to inform generalizability of these results and increase understanding of healthy living, aging, and cardiometabolic risk.

## ARTICLE INFORMATION

**Accepted for Publication:** July 26, 2017.

**Published Online:** September 20, 2017.  
doi:10.1001/jamacardio.2017.3145

**Author Affiliations:** Cardiovascular Research Center, Massachusetts General Hospital, Boston (Shah, Yeri, Das); Department of Cardiology, University of Michigan, Ann Arbor (Murthy); Department of Statistics, Boston University, Boston, Massachusetts (Massaro); Department of Mathematics and Statistics, Boston University, Boston, Massachusetts (D'Agostino); University of Massachusetts, Worcester (Freedman); Framingham Heart Study, Framingham, Massachusetts (Long, Fox, Benjamin, Vasan); Section of Gastroenterology, Department of Medicine, Boston University School of Medicine, Boston, Massachusetts (Long); Merck Research Laboratories, Boston, Massachusetts (Fox); Cardiology and Preventive Medicine and Epidemiology Sections, Boston University School of Medicine, and Department of Epidemiology, Boston University School of Public Health, Boston, Massachusetts (Benjamin); Cardiology Section, Department of Medicine, Boston VA Healthcare, Boston, Massachusetts (O'Donnell); Associate Editor, *JAMA Cardiology* (O'Donnell); Department of Radiology, Massachusetts General Hospital, Boston (Hoffmann).

**Author Contributions:** Drs Shah and Hoffmann had access to all of the data in the study and take responsibility for the integrity of the data and the accuracy of the data analysis. Drs Shah, Yeri, and Murthy contributed equally.

**Study concept and design:** Shah, Yeri, Murthy, D'Agostino, Freedman, Fox, Benjamin, Vasan, O'Donnell, Hoffmann.

**Acquisition, analysis, or interpretation of data:** Shah, Yeri, Murthy, Massaro, D'Agostino, Freedman, Long, Das, Benjamin, Vasan, O'Donnell, Hoffmann.

**Drafting of the manuscript:** Shah, Yeri, Freedman, Hoffmann.

**Critical revision of the manuscript for important intellectual content:** Shah, Yeri, Murthy, Massaro, D'Agostino, Long, Fox, Das, Benjamin, Vasan, O'Donnell, Hoffmann.

**Statistical analysis:** Shah, Yeri, Massaro, D'Agostino.  
**Obtained funding:** Freedman, Fox, Das, Vasan, O'Donnell.

**Administrative, technical, or material support:** Vasan, Hoffmann.

**Study supervision:** Shah, Freedman, Das, Hoffmann.

**Conflict of Interest Disclosures:** All authors have completed and submitted the ICMJE Form for Disclosure of Potential Conflicts of Interest. Dr Murthy reported stockholdings in General Electric. Dr Massaro reported grants from the National Heart, Lung, and Blood Institute. Dr Long reported grants from Echosens. Dr Fox is a full-time employee of Merck. Dr Das reported grants from the National Institutes of Health. Dr Benjamin reported grants from the National Institutes of Health; National Heart, Lung, and Blood Institute; and American Heart Association as well as personal fees from the American Heart Association, National Institutes of Health, and National Center for Biotechnology Information. No other disclosures were reported.

**Funding/Support:** This research was conducted in part using data and resources from the Framingham

Heart Study of the National Heart, Lung, and Blood Institute of the National Institutes of Health and Boston University School of Medicine (HHSN268201500001 and N01-HC 25195 to Dr Vasan). Dr Shah is funded by Career Development Award K23-HL127099 from the National Institutes of Health. Drs Shah and Murthy are funded by grant R01-HL136685 from the National Institutes of Health. Dr Benjamin is funded by grants 2R01HL092577 and 1R01HL128914 from the National Institutes of Health.

**Role of the Funder/Sponsor:** The funders had no role in the design and conduct of the study; collection, management, analysis, and interpretation of the data; preparation, review, or approval of the manuscript; and decision to submit the manuscript for publication.

**Disclaimer:** Dr O'Donnell is an Associate Editor of *JAMA Cardiology*, but he was not involved in any of the decisions regarding review of the manuscript or its acceptance.

## REFERENCES

- Alnabelsi TS, Alhamshari Y, Mulki RH, et al. Relation between epicardial adipose and aortic valve and mitral annular calcium determined by computed tomography in subjects aged  $\geq 65$  years. *Am J Cardiol*. 2016;118(7):1088-1093.
- Mahabadi AA, Lehmann N, Möhlenkamp S, et al; Heinz Nixdorf Investigative Group. Noncoronary measures enhance the predictive value of cardiac CT above traditional risk factors and CAC score in the general population. *JACC Cardiovasc Imaging*. 2016;9(10):1177-1185.
- Wassel CL, Laughlin GA, Saad SD, et al. Associations of abdominal muscle area with 4-year change in coronary artery calcium differ by ethnicity among post-menopausal women. *Ethn Dis*. 2015;25(4):435-442.
- Whelton SP, Silverman MG, McEvoy JW, et al. Predictors of long-term healthy arterial aging: coronary artery calcium nondevelopment in the MESA Study. *JACC Cardiovasc Imaging*. 2015;8(12):1393-1400.
- Handy CE, Desai CS, Dardari ZA, et al. The association of coronary artery calcium with noncardiovascular disease: the Multi-Ethnic Study of Atherosclerosis. *JACC Cardiovasc Imaging*. 2016;9(5):568-576.
- Kuller LH, Lopez OL, Mackey RH, et al. Subclinical cardiovascular disease and death, dementia, and coronary heart disease in patients 80+ years. *J Am Coll Cardiol*. 2016;67(9):1013-1022.
- McClelland RL, Chung H, Detrano R, Post W, Kronmal RA. Distribution of coronary artery calcium by race, gender, and age: results from the Multi-Ethnic Study of Atherosclerosis (MESA). *Circulation*. 2006;113(1):30-37.
- Hoffmann U, Massaro JM, D'Agostino RB Sr, Kathiresan S, Fox CS, O'Donnell CJ. Cardiovascular event prediction and risk reclassification by coronary, aortic, and valvular calcification in the Framingham Heart Study. *J Am Heart Assoc*. 2016;5(2):e003144.
- Abraham TM, Pedley A, Massaro JM, Hoffmann U, Fox CS. Association between visceral and subcutaneous adipose depots and incident cardiovascular disease risk factors. *Circulation*. 2015;132(17):1639-1647.
- Britton KA, Massaro JM, Murabito JM, Kreger BE, Hoffmann U, Fox CS. Body fat distribution, incident cardiovascular disease, cancer, and all-cause mortality. *J Am Coll Cardiol*. 2013;62(10):921-925.
- Spahillari A, Mukamal KJ, DeFilippi C, et al. The association of lean and fat mass with all-cause mortality in older adults: the Cardiovascular Health Study. *Nutr Metab Cardiovasc Dis*. 2016;26(11):1039-1047.
- Moore AZ, Caturegli G, Metter EJ, et al. Difference in muscle quality over the adult life span and biological correlates in the Baltimore Longitudinal Study of Aging. *J Am Geriatr Soc*. 2014;62(2):230-236.
- Therkelsen KE, Pedley A, Hoffmann U, Fox CS, Murabito JM. Intramuscular fat and physical performance at the Framingham Heart Study. *Age (Dordr)*. 2016;38(2):31.
- Ma J, Hwang SJ, McMahon GM, et al. Mid-adulthood cardiometabolic risk factor profiles of sarcopenic obesity. *Obesity (Silver Spring)*. 2016;24(2):526-534.
- Nikolov J, Spira D, Aleksandrova K, et al. Adherence to a Mediterranean-style diet and appendicular lean mass in community-dwelling older people: results from the Berlin Aging Study II. *J Gerontol A Biol Sci Med Sci*. 2016;71(10):1315-1321.
- Meyer A, Salewsky B, Spira D, Steinhagen-Thiessen E, Norman K, Demuth I. Leukocyte telomere length is related to appendicular lean mass: cross-sectional data from the Berlin Aging Study II (BASE-II). *Am J Clin Nutr*. 2016;103(1):178-183.
- Eibich P, Buchmann N, Kroh M, et al. Exercise at different ages and appendicular lean mass and strength in later life: results from the Berlin Aging Study II. *J Gerontol A Biol Sci Med Sci*. 2016;71(4):515-520.
- Post W, Bielak LF, Ryan KA, et al. Determinants of coronary artery and aortic calcification in the Old Order Amish. *Circulation*. 2007;115(6):717-724.
- Wang TJ, Gona P, Larson MG, et al. Multiple biomarkers for the prediction of first major cardiovascular events and death. *N Engl J Med*. 2006;355(25):2631-2639.
- Shah SJ, Katz DH, Selvaraj S, et al. Phenomapping for novel classification of heart failure with preserved ejection fraction. *Circulation*. 2015;131(3):269-279.
- Frizzell JD, Liang L, Schulte PJ, et al. Prediction of 30-day all-cause readmissions in patients hospitalized for heart failure: comparison of machine learning and other statistical approaches. *JAMA Cardiol*. 2017;2(2):204-209.
- Speliotes EK, Massaro JM, Hoffmann U, et al. Fatty liver is associated with dyslipidemia and dysglycemia independent of visceral fat: the Framingham Heart Study. *Hepatology*. 2010;51(6):1979-1987.
- Feinleib M, Kannel WB, Garrison RJ, McNamara PM, Castelli WP. The Framingham Offspring Study: design and preliminary data. *Prev Med*. 1975;4(4):518-525.

24. Fraley C, Raftery AE. Model-based clustering, discriminant analysis, and density estimation. *J Am Stat Assoc.* 2002;97:611-631. doi:10.1198/016214502760047131
25. Pencina MJ, D'Agostino RB. Overall C as a measure of discrimination in survival analysis: model specific population value and confidence interval estimation. *Stat Med.* 2004;23(13):2109-2123.
26. Pencina MJ, D'Agostino RB Sr, D'Agostino RB Jr, Vasan RS. Evaluating the added predictive ability of a new marker: from area under the ROC curve to reclassification and beyond. *Stat Med.* 2008;27(2):157-172.
27. D'Agostino RB Sr, Vasan RS, Pencina MJ, et al. General cardiovascular risk profile for use in primary care: the Framingham Heart Study. *Circulation.* 2008;117(6):743-753.
28. Cureton E, D'Agostino R. *Factor Analysis: An Applied Approach.* Hillsdale, NJ: Lawrence Erlbaum Associates; 1983.
29. Gerstenblith G, Frederiksen J, Yin FC, Fortuin NJ, Lakatta EG, Weisfeldt ML. Echocardiographic assessment of a normal adult aging population. *Circulation.* 1977;56(2):273-278.
30. Cheng S, Xanthakis V, Sullivan LM, et al. Correlates of echocardiographic indices of cardiac remodeling over the adult life course: longitudinal observations from the Framingham Heart Study. *Circulation.* 2010;122(6):570-578.
31. Strait JB, Lakatta EG. Aging-associated cardiovascular changes and their relationship to heart failure. *Heart Fail Clin.* 2012;8(1):143-164.
32. Bays HE. Adiposopathy is "sick fat" a cardiovascular disease? *J Am Coll Cardiol.* 2011;57(25):2461-2473.
33. Al Rifai M, Silverman MG, Nasir K, et al. The association of nonalcoholic fatty liver disease, obesity, and metabolic syndrome, with systemic inflammation and subclinical atherosclerosis: the Multi-Ethnic Study of Atherosclerosis (MESA). *Atherosclerosis.* 2015;239(2):629-633.
34. Abbasi SA, Hundley WG, Bluemke DA, et al. Visceral adiposity and left ventricular remodeling: the Multi-Ethnic Study of Atherosclerosis. *Nutr Metab Cardiovasc Dis.* 2015;25(7):667-676.
35. VanWagner LB, Wilcox JE, Colangelo LA, et al. Association of nonalcoholic fatty liver disease with subclinical myocardial remodeling and dysfunction: a population-based study. *Hepatology.* 2015;62(3):773-783.
36. VanWagner LB, Ning H, Lewis CE, et al. Associations between nonalcoholic fatty liver disease and subclinical atherosclerosis in middle-aged adults: the Coronary Artery Risk Development in Young Adults Study. *Atherosclerosis.* 2014;235(2):599-605.